JOURNAL OF CATALYSIS 143, 286–298 (1993)

Oxidative Coupling of Methane over Oxide-Supported Barium Catalysts

DHAMMIKE DISSANAYAKE, JACK H. LUNSFORD, AND MICHAEL P. ROSYNEK[1]

Department of Chemistry, Texas A & M University, College Station, Texas 77843

Received March 11, 1993; revised May 5, 1993

The effects of barium loading level and support basicity on the activity and C_{2+} selectivity for oxidative coupling of methane were examined for MgO-, CaO-, ZnO-, and Al_2O_3-supported Ba catalysts. The nature and distribution of catalyst surface species were characterized by XPS and ISS spectroscopic techniques, which indicated that there is no direct correlation between support basicity and oxidative coupling activity. However, catalysts containing sufficiently high Ba loadings are more easily poisoned by carbon dioxide than those with low Ba contents, due to increased stability of a $BaCO_3$ phase. With supports of low basicity, or when the Ba is uniformly distributed on the catalyst support, the susceptibility to carbon dioxide poisoning is minimized. XPS characterization of the Ba/MgO catalysts confirmed that oxidative coupling activity is directly related to the capability of the catalyst to form surface O_2^{2-} ions existing in a BaO_2 phase that is sustained under reaction conditions by the presence of molecular O_2. With a 2 mol% Ba/MgO catalyst, a C_{2+} selectivity of 80% at a CH_4 conversion of 17% was achieved using a $CH_4 : O_2 = 10 : 1$ reactant mixture at 800°C and a total reagent pressure of 1 atm.

INTRODUCTION

The partial oxidation of methane with molecular O_2 to produce C_{2+} hydrocarbon products has been extensively investigated during the past several years (*1*). Because of the stability of the C–H bond in methane, relatively high temperatures, i.e., >700°C, are typically required to produce appreciable concentrations of radicals with most oxides. The most generally accepted mechanism for the formation of $CH_3\cdot$ radicals on oxides involves the abstraction of a hydrogen atom from either gaseous (*2–5*) or adsorbed (*6*) CH_4 by a partially reduced surface oxygen species (e.g., O^-, O_2^-, or O_2^{2-}). The resulting $CH_3\cdot$ species may either couple in the gas phase to form the desired ethane product or undergo secondary reactions with gaseous O_2 or with surface oxygen species to generate undesirable CO_x byproducts. Ethane, the primary reaction product (and its dehydrogenation product, ethylene) may also undergo secondary oxidation to CO_x. The surface OH species generated as a result of H abstraction from CH_4 are removed as water, forming surface vacancies and O^{2-} species on the oxide. The active sites are subsequently regenerated by gas-phase O_2 (*2*) or by adsorbed molecular O_2 (*6*).

Among the wide variety of oxide catalysts that have been studied for the partial oxidation of methane (*1, 7–11*), most of those that are both active for methane conversion and selective for the formation of C_{2+} products, such as alkaline earth and lanthanide oxides, possess an intrinsically basic nature (*2, 6, 12, 13*). As a result, several authors have attempted to correlate basicity with C_{2+} product selectivity for oxidative coupling catalysts (*14–17*). Sokolovskii *et al.*, for example, have investigated the relationship between the intrinsic basicity of the alkaline earth oxides, as measured by benzoic acid adsorption, and their C_2 product selectivities for methane oxidation (*17*). They observed that C_2 selectivity increased with increasing basicity, in the order BaO > SrO > CaO > MgO > BeO. Similarly, Luns-

[1] To whom correspondence should be addressed.

0021-9517/93 $5.00

ford and co-workers reported that C_{2+} yields over several lanthanide oxides at 600–700°C decreased in the order $Nd_2O_3 > La_2O_3 > Sm_2O_3 > Dy_2O_3 \gg CeO_2$, which correlates approximately with the decreasing basicity of these oxides (*18*). It is significant that, except for the order of Nd_2O_3 and La_2O_3 being reversed, the production of $CH_3\cdot$ radicals over these oxides follows the same sequence. It is also noteworthy that the multivalent CeO_x, PrO_x, and TbO_x oxides are ineffective for $CH_3\cdot$ radical generation and, although quite active for methane conversion, result only in CO_x formation and exhibit virtually no selectivity for C_{2+} products.

Several surface oxygen species have been proposed as active sites for methane activation. In the case of Li/MgO, for example, convincing evidence exists for the involvement of Li^+O^- centers in the initial formation of $CH_3\cdot$ radicals (*2, 3*). On various other oxides, superoxide (O_2^-) and peroxide (O_2^{2-}) sites have been suggested (*19, 20*). The uncatalyzed (i.e., stoichiometric) reaction of methane with the peroxides of Na, Sr, and Ba, in fact, has been reported to produce C_2 products (*7, 21*). The activity of molten $Ba(OH)_2$ has also been attributed to a peroxide species (*22*). Because of their relatively high C_{2+} selectivities and variety of oxygen-containing phases, barium compounds have been extensively studied as catalysts for the partial oxidation of methane. In addition to the BaO and BaO_2 phases that may exist under oxidative coupling conditions, a study by Aika *et al.* indicated that $BaCO_3$ may also be a catalytically active component (*23*). Addition of K_2CO_3 promoter served to increase the C_{2+} yield, possibly because of the comparable ionic radii of K^+ and Ba^{2+}. Yamashita *et al.* observed that addition of Ba to La_2O_3 resulted in an improvement in both catalytic activity and C_2 selectivity, with activities being directly proportional to Ba content (*24*). The active phase was suggested to be either BaO_2 or the O^- ions that are generated by breaking the O–O bond of the O_2^{2-} species. Zhang *et al.* ascribed the increased catalytic activity of Ba/La_2O_3 to a type of structural defect site occurring at the $La_2O_3/BaCO_3$ interface. This defect was identified by ESR and Raman spectroscopies (*10*). Cameron and coworkers proposed that the carbonate-assisted formation of an active oxygen species (via generation of CO_4^{2-} and O^-) is responsible for the oxidative coupling activity of Ba/La_2O_3 (*25*).

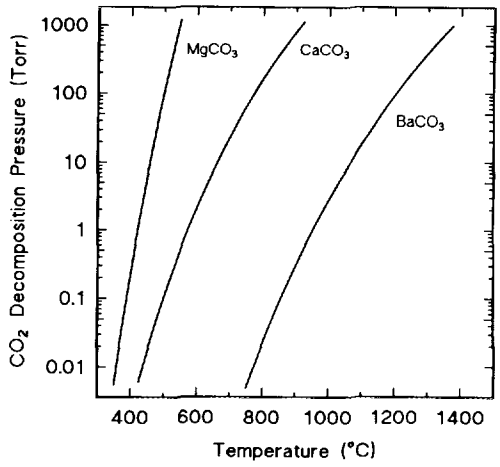

FIG. 1. Effect of temperature on CO_2 decomposition pressures of alkaline earth carbonates. (Data from Ref. (*26*), fitted to equations of the form $P = \exp(A/T + B)$.)

Because of their relatively high basicities, Ba–O catalysts are susceptible to attack by CO_2. The formation of CO_2 inevitably accompanies that of the desired coupling products, and results in the generation of a surface $BaCO_3$ phase. Although $BaCO_3$ may possess some activity for the coupling reaction (*23*), the presence of significant amounts of it causes a decrease in overall methane conversion. As shown in Fig. 1, the decomposition pressure of $BaCO_3$ at 800°C is only 0.01 Torr of CO_2. Thus, under typical oxidative coupling conditions, the CO_2 partial pressure may easily be sufficient to maintain a $BaCO_3$ phase. It is possible, however, that if CO_2 is produced primarily via homogeneous gaseous reactions, its localized concentration near the catalyst surface in a typical flow reactor may be much

less than that in the gas phase. Hence, the role of CO_2 in influencing the behavior of oxidative coupling catalysts warrants further investigation.

The present study was performed to determine the behaviors of a series of Ba/MgO catalysts and of Ba/CaO, Ba/ZnO, and Ba/Al_2O_3 for the partial oxidation of methane. Correlations between the catalytic activities and selectivities of these materials and their surface properties, as determined by X-ray photoelectron (XPS) and ion scattering (ISS) spectroscopic characterizations, were investigated. In addition, the susceptibility to CO_2 poisoning was explored for a series of Ba/MgO catalysts having Ba loadings in the range 0.2–25 mol%.

EXPERIMENTAL

Materials

All reagents used for catalyst preparation were ACS certified grade. A series of Ba/MgO catalysts containing varying amounts of barium in the range 0.2 to 25 mol% were prepared by adding 10 g of MgO to 50–60 ml of deionized water that contained an appropriate concentration of dissolved $Ba(NO_3)_2$. Each resultant slurry was stirred overnight at room temperature, evaporated to dryness, and crushed into 20–45 mesh granules. The catalyst particles were then calcined in air at 800°C for 1 h prior to use. The Ba/CaO, Ba/ZnO, and Ba/Al_2O_3 catalysts, containing 2.0, 2.0, and 4.0 mol% Ba, respectively, were synthesized in a similar manner. The BET-N_2 surface areas of the pure supports and synthesized catalysts are summarized in Table 1. Methane (99.99%) from Matheson Co. and oxygen (99.9%), helium (99.995%), and carbon dioxide (99.9%) from Airco were used without further purification.

TABLE 1

Surface Areas of Catalysts and Supports (m^2/g)

Catalyst/support	Fresh[a]	Used[b]
MgO	68	36
Ba/MgO (mol% Ba)		
0.2	41	32
0.5	21	17
1.0	21	13
2.0	9.3	7.7
4.0	8.8	4.4
8.0	8.1	3.3
15.0	2.1	1.0
25.0	3.0	1.0
$BaCO_3$	3.0	1.0
CaO	17	9.6
Ba/CaO (2 mol% Ba)	9.7	7.4
ZnO	3.3	1.0
Ba/ZnO (2 mol% Ba)	1.7	1.0
Al_2O_3	294	105
Ba/Al_2O_3 (4 mol% Ba)	81	77

[a] After initial treatment in O_2 at 800°C for 10 h.
[b] Following exposure to a $CH_4:O_2:He = 5:1:6$ reaction mixture for 12 h at 800°C.

Procedures

All catalytic experiments were performed using a downflow tubular quartz reactor having an internal diameter of 2.85 mm. The catalyst particles were secured in the reactor between quartz wool plugs, and a 5.0-cm layer of quartz chips, located on top of the catalyst bed, served as the preheating zone. The temperature of the reactor was controlled by a proportional band temperature controller, using a chromel–alumel sensing thermocouple that was directly attached to the outside of the reactor at the midpoint of the catalyst bed. Measurements of the activity and selectivity of the various catalysts for methane oxidation were performed at 750–850°C under nearly differential conditions, in which oxygen and methane conversions were typically less than 20 and 10%, respectively. These conditions were achieved by using small amounts (12.5 mg) of catalyst and high reactant/diluent flow rates ($CH_4:O_2:He = 100:20:200$ cm^3/min. In the cases of those catalysts having very low activity (viz., pure MgO, $BaCO_3$, 15 mol% Ba/MgO, and 25 mol% Ba/MgO), larger amounts (25 to 50 mg) of catalyst were employed. The carbon dioxide poisoning experiments were performed at 850°C, using a feed mixture of $CH_4:O_2 = 50:5$ cm^3/min, with 2 to 20 cm^3/min of CO_2 added to achieve the desired CO_2 partial pressure.

The total flow rate was maintained at 120 cm^3/min by appropriate adjustment of the diluent He flow rate. The products of the reaction were analyzed by gas chromatography, using a Chromosorb 107 column for separation of carbon dioxide and C_2 hydrocarbons and a 13X molecular sieve column on which separation of oxygen, carbon monoxide, and methane was achieved.

Temperature-programmed desorption (TPD) of adsorbed CO_2 was performed using a greaseless micro-volume system consisting of stainless steel valves and fittings, a thermal conductivity detector, and a U-shaped quartz reactor containing 100 mg of catalyst. Previously calcined samples were heated to 970°C in flowing He, cooled in pure flowing CO_2 to 120°C, and then flushed with He for 3 h. The sample temperature was increased at 16°C/min under a He flow of 30 ml/min to 970°C, and then maintained isothermally at the latter temperature, if necessary, until desorption was completed.

XPS and ISS spectra were acquired using a Perkin–Elmer Model 5500 spectrometer equipped with a dual Mg–Zr anode and an external stainless steel reaction system that allowed thermal and chemical pretreatments of samples at temperatures up to 600°C, followed by direct *in situ* introduction into the UHV analysis chamber. Samples requiring gas treatment and/or evacuation at temperatures >600°C were treated in a separate quartz reactor system that allowed *in situ* transfer of the ceramic holder containing the treated sample into an O-ring-sealed stainless steel transport vessel that was attached to the system. The removable vessel was then fitted directly to an evacuable inlet port on the spectrometer, allowing completely anaerobic transfer of externally treated samples into the instrument's UHV analysis chamber. All samples were prepared in the form of pressed wafers and, prior to spectral analyses, were given thermal and chemical treatments that duplicated those employed in the catalytic reaction experiments. Spectra were recorded for samples both after initial treatment in O_2 at 800°C (fresh) and after subsequent exposure to the $CH_4 : O_2$: He reaction mixture (used). In a typical XPS data acquisition, a pass energy of 58.7 eV, step increment of 0.125 eV, and Mg anode powder of 300 W provided an optimum combination of resolution and data collection time. Photoelectrons were collected at an angle of 45° to the sample surface for 7 min in each spectral region scanned. All measured binding energies were adjusted with respect to the Ba $3d_{5/2}$ peak at 779.7 eV. The latter was calibrated in selected samples by referencing it to the Au $4f_{7/2}$ peak at 83.8 eV resulting from sputter deposition of a small Au spot onto the sample. Near-surface compositions were calculated from peak areas in each spectral region, using appropriate sensitivity factors for each line. ISS spectra were obtained using $^3He^+$ ions at a scattering angle of 134.5° and 1 kV accelerating potential.

RESULTS AND DISCUSSION

Reaction Results for Ba/MgO Catalysts

In order to allow sufficient time for activities and C_2 selectivities to stabilize, all catalyst samples were exposed to the $CH_4 : O_2$: He reaction mixture for at least 12 h at 800°C prior to acquiring catalytic reaction data. Specific activities of all catalysts were calculated from reaction rates obtained under differential conditions. Figures 2 and 3 display the specific activities and C_2 selectivities of the various Ba/MgO catalysts as a function of Ba loading for three reaction temperatures in the range 750–850°C. (The catalyst represented in both figures as containing 100% Ba originated as pure $BaCO_3$, but was partially transformed into BaO_x by the initial O_2 treatment at 800°C, as evidenced by the CO_2 poisoning results to be described below.) At all reaction temperatures studied, specific activity increased with increasing Ba loading up to 4 mol% of Ba, and then declined for higher Ba contents. Similarly, although *total* C_2 selectivities increased continuously with increasing Ba content, the ethylene/

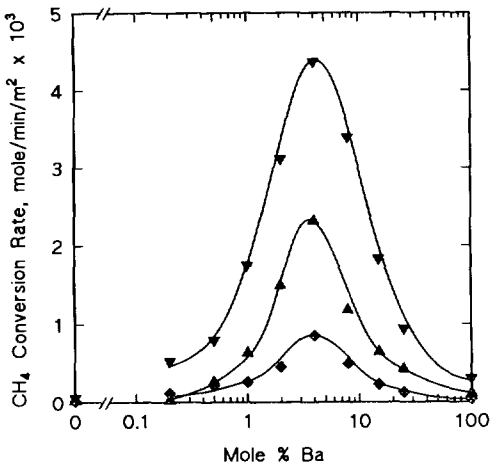

FIG. 2. Specific activities of Ba/MgO catalysts at $CH_4:O_2 = 5:1$. ◆, 750°C; ▲, 800°C; and ▼, 850°C.

ethane ratio in the C_2 products appeared to pass through a maximum at approximately the same Ba loading as that observed for methane oxidation, as shown in Table 2. In all cases, both the specific activity and C_2 selectivity for a given Ba loading increased with increasing reaction temperature. Since the activities shown in Fig. 2 have already been corrected for variations in surface area among the various catalysts (Table 1), the maximum in activity observed at a Ba loading of 4 mol% may be due to differing susceptibilities to poisoning by the carbon dioxide produced during the reaction.

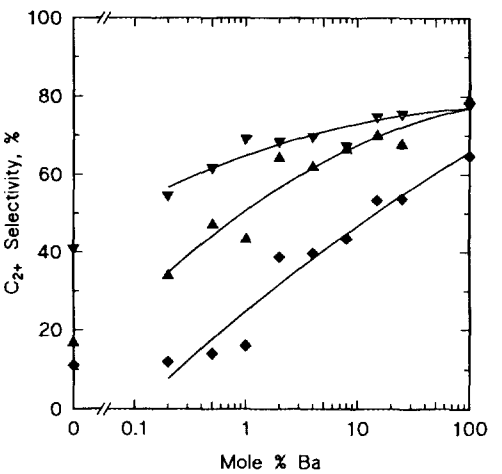

FIG. 3. C_{2+} product selectivities of Ba/MgO catalysts at $CH_4:O_2 = 5:1$. ◆, 750°C; ▲, 800°C; and ▼, 850°C.

TABLE 2

Reaction Results for Ba/MgO Catalysts

Catalyst	E_a (kcal/mol)[a]		S.V. (ml/g/h × 10)	C_2H_4/C_2H_6 at 850°C[a]	
	1	2		1	2
MgO	30		2.2	0.21	
0.2% Ba/MgO	34		15.4	0.25	
0.5% Ba/MgO	34	48	15.4	0.21	0.16
1.0% Ba/MgO	34		15.4	0.33	
2.0% Ba/MgO	39		15.4	0.32	
4.0% Ba/MgO	39	49	15.4	0.24	0.21
8.0% Ba/MgO	43		15.4	0.15	
15.0% Ba/MgO	43	55	7.7	0.19	0.15
25.0% Ba/MgO	43		7.7	0.18	
$BaCO_3$	57		3.8	0.07	

[a] 1 = without addition of CO_2 to the reactant stream; 2 = with addition of 13 Torr of CO_2 to the reactant stream.

The effect of carbon dioxide on the activity and the C_2 selectivity of the catalysts was further investigated by adding varying amounts of CO_2 to a 10 : 1 $CH_4:O_2$ reaction mixture at 850°C, with the He diluent flow rate appropriately adjusted to maintain a total flow rate of 120 cm^3/min in each case. Unlike the experiments shown in Figs. 1 and 2, these reactions, in general, were not performed under differential conditions, since O_2 conversions exceeded 50% in most cases. Methane conversions and C_2 selectivities as a function of total CO_2 partial pressure (i.e., that added plus that produced by the oxidation reaction) are shown for selected Ba/MgO compositions in Figs. 4 and 5, respectively. In both of these figures, the data point corresponding to the lowest CO_2 partial pressure for each catalyst was that obtained with no added CO_2. It can be seen from Fig. 4 that the activities of pure MgO and of Ba/MgO catalysts containing up to 1 mol% Ba are much less affected by carbon dioxide than are those of the samples containing 2 mol% Ba or more. The loss of activity in each case may be attributed to the formation of a stable surface $BaCO_3$ phase, which can be maintained at 850°C by local CO_2 pressures as low as ~0.05 Torr (Fig. 1). The XPS results to be presented below

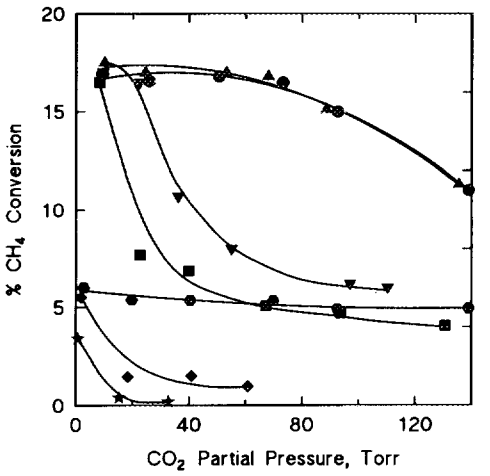

FIG. 4. Effect of CO_2 partial pressure on CH_4 conversion over Ba/MgO catalysts at 850°C and $CH_4:O_2$ = 10:1. , MgO; ▲, 0.5 mol% Ba; ●, 1 mol% Ba; ▼, 2 mol% Ba; ■, 8 mol% Ba; ◆, 25 mol% Ba; and ★, $BaCO_3$.

confirm that the catalysts which were most sensitive to poisoning by CO_2 contained significant concentrations of surface carbonate species after use. It is particularly noteworthy that, in the absence of added CO_2, the catalyst which originated as pure $BaCO_3$ exhibited activity for CH_4 conversion that was comparable to that of pure MgO. Unlike MgO, however, which does not form a stable carbonate phase under these conditions (Fig. 1) and whose activity is consequently unaffected by added CO_2, the $BaCO_3$-based catalyst was completely poisoned by the addition of even a small amount of CO_2 to the reactant stream. This observation indicates that the O_2 pretreatment at 800°C may cause decomposition of at least a small amount of the initial $BaCO_3$ into an active surface BaO_x phase, which is subsequently converted back into inactive $BaCO_3$ when CO_2 is added to the reactant stream. Although CO_2 is, of course, generated during the CH_4 oxidation reaction, the *initial* portion of the catalyst bed in a flow reactor may remain active because the CO_2 produced is quickly swept away by the reactant stream, resulting in an effective CO_2 partial pressure near the catalyst surface in this region of the bed that is insufficient to maintain a stable carbonate phase. By contrast, when CO_2 is present in the reactant stream, even the initial portion of the catalyst bed is exposed to a CO_2 partial pressure that is sufficient to maintain the inactive $BaCO_3$ phase.

C_2 product selectivities over the Ba/MgO catalysts (Fig. 5) were affected much less by CO_2 than were the corresponding activities. Those catalysts containing the lowest Ba loadings (0.5, 1, and 2 mol%), in fact, exhibited slight increases in C_2 selectivity at total CO_2 pressures up to ~60 Torr, before decreasing somewhat at higher CO_2 pressures. By contrast, selectivities over catalysts containing high Ba loadings (8 mol% or more) decreased even for low pressures of added CO_2, up to ~60 Torr, but then remained essentially constant at higher CO_2 partial pressures. The C_2 selectivity over pure MgO also decreased initially with increasing CO_2 partial pressure, and then remained constant at CO_2 pressures of ~60 Torr or greater. The results in Figs. 4 and 5 demonstrate that the 2 mol% Ba/MgO, in particular, is a very effective catalyst for the oxidative coupling reaction. Few catalysts have

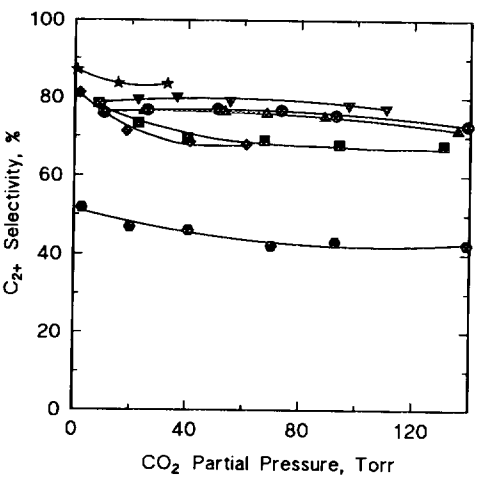

FIG. 5. Effect of CO_2 partial pressure on C_{2+} selectivity over Ba/MgO catalysts at 850°C and $CH_4:O_2$ = 10:1. , MgO; ▲, 0.5 mol% Ba; ●, 1 mol% Ba; ▼, 2 mol% Ba; ■, 8 mol% Ba; ◆, 25 mol% Ba; and ★, $BaCO_3$.

been previously reported to give C_{2+} selectivities of 80% at conversions as high as 17% and at total *reagent* partial pressures of 1 atm (i.e., without an inert diluent). Moreover, this catalyst is very stable, with CH_4 conversion and C_{2+} selectivity remaining undiminished after 50 h of continuous operation.

The effect of Ba loading on sensitivity to poisoning by CO_2 is also reflected by variations in the apparent activation energies observed for the oxidative coupling reaction over the various Ba/MgO catalysts, as shown in Table 2. The E_a values listed were measured under the same differential reaction conditions as those used to obtain the data in Figs. 2 and 3. The apparent activation energies increased gradually with increasing Ba content, indicative of increasing susceptibility to the CO_2 produced during the reaction, with the highest activation energy being observed for the catalyst which originated as pure $BaCO_3$. When a partial pressure of 13 Torr of CO_2 (an amount approximately equal to that produced in a typical catalytic experiment under these conditions) was added to the reactant stream, the activation energy for each Ba loading increased further. At sufficiently high concentrations of added CO_2, the behavior of each catalyst approached that of pure $BaCO_3$. Although the inherent basicity of a Ba/MgO catalyst, as determined by its ability to retain adsorbed CO_2, may be dependent on its Ba loading, basicity determined in this manner would not be expected to pass through a maximum at a specific Ba content. Indeed, TPD measurements revealed that the desorption temperature of adsorbed CO_2 increased with Ba loading, but only up to a Ba content of 2 mol%. The TPD behaviors at all higher Ba loadings were virtually identical to that of pure $BaCO_3$, as shown by the representative thermograms in Fig. 6. Hence, variations in catalyst basicity, at least when measured by CO_2 adsorption strength, cannot be used to explain the maximum activities observed in Fig. 2 for a Ba loading of 4 mol%.

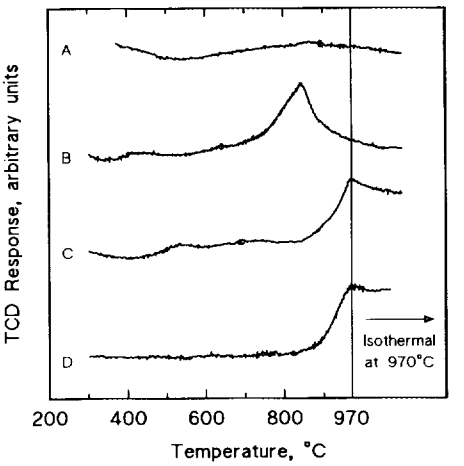

FIG. 6. Temperature-programmed desorption of CO_2 (heating rate = 16°C/min to 970°C): (A) MgO, (B) 0.5 mol% Ba/MgO, (C) 2.0 mol% Ba/MgO, and (D) $BaCO_3$.

Reaction Results for Ba/CaO, Ba/ZnO, and Ba/Al_2O_3 Catalysts

The influence of variations in catalyst basicity and resulting surface carbonate formation on oxidative coupling properties was further investigated by comparing the methane oxidation behaviors of CaO-, ZnO-, and Al_2O_3-supported Ba to that of Ba/MgO. Results of carbon dioxide poisoning experiments, analogous to those depicted in Figs. 4 and 5, are shown in Figs. 7 and 8 for 2 mol% Ba/CaO and Ba/ZnO and 4 mol% Ba/Al_2O_3, as well as for each of the pure oxide supports. Data for 2 mol% Ba/MgO from Figs. 4 and 5 are also included for comparison purposes. As in the latter two figures, the data point corresponding to the lowest CO_2 partial pressure for each catalyst was that obtained with no added CO_2, while the other data points for each catalyst include both the CO_2 produced during the reaction and that added to the reactant stream. Although the activities of the four pure oxide catalysts differed considerably, neither the activity nor C_2 selectivity of any of them was influenced significantly by variations in total CO_2 partial pressure. Similarly, among the Ba-containing catalysts, activities of both Ba/CaO and Ba/Al_2O_3 were also largely unaffected by variations in CO_2

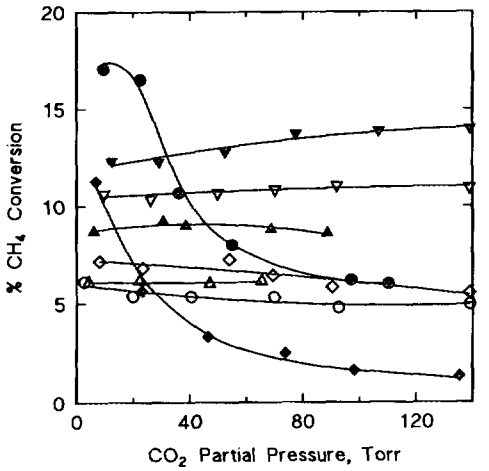

FIG. 7. Effect of CO_2 partial pressure on CH_4 conversion over supported Ba catalysts at 850°C and CH_4: O_2 = 10:1. ○, MgO; ●, 2 mol% Ba/MgO; ▽, CaO; ▼, 2 mol% Ba/CaO; ◇, ZnO; ◆, 2 mol% Ba/ZnO; △, Al_2O_3; and ▲, 4 mol% Ba/Al_2O_3.

level. By contrast, however, the activity of the Ba/ZnO catalyst decreased markedly with increasing CO_2 pressure, a behavior which closely resembled that observed for Ba/MgO at the same Ba loading. C_2 selectivities for the Ba/ZnO and Ba/Al_2O_3 catalysts decreased somewhat with increasing CO_2

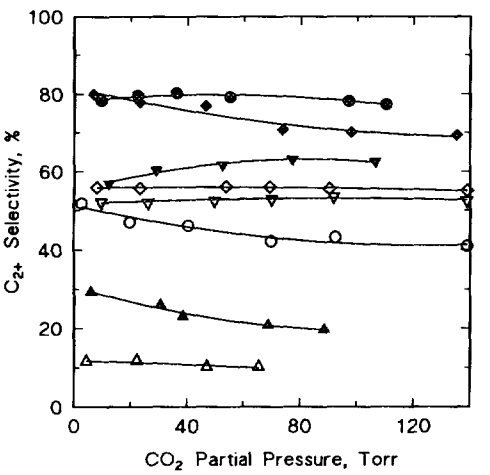

FIG. 8. Effect of CO_2 partial pressure on C_{2+} selectivity over supported Ba catalysts at 850°C and CH_4: O_2 = 10:1. ○, MgO; ●, 2 mol% Ba/MgO; ▽, CaO; ▼, 2 mol% Ba/CaO; ◇, ZnO; ◆, 2 mol% Ba/ZnO; △, Al_2O_3; and ▲, 4 mol% Ba/Al_2O_3.

partial pressure, while those for Ba/MgO and Ba/CaO were virtually unaffected.

It should be noted that pure CaO itself is a fairly active and selective catalyst for the oxidative coupling reaction. XPS analysis of the used Ba/CaO catalyst, however, revealed that all of the Ba in this material existed as $BaCO_3$, even when no CO_2 was added to the reactant stream. Thus, the presence of added CO_2 would not be expected to cause a decrease in activity due to surface carbonate formation, such as that observed for Ba/MgO. However, a fraction of the surface Ba may still be available in an active form, even in the presence of added CO_2, resulting in the observed higher activity for Ba/CaO than for pure CaO. The activity of Ba/ZnO, on the other hand, although higher than that of pure ZnO in the absence of added CO_2, decreased quickly with increasing CO_2 partial pressure to a level much lower than that of ZnO even at relatively low levels of added CO_2. This behavior is similar to that observed for Ba/MgO at sufficiently high Ba loadings, e.g., 25 mol% Ba/MgO (Fig. 4). XPS analyses showed that the surfaces of catalysts demonstrating this type of behavior are almost completely covered with Ba, with little exposure of the underlying support oxide. Hence, addition of carbon dioxide causes increasing formation of a surface $BaCO_3$ phase, and the activities of these catalysts approach that of pure $BaCO_3$. By contrast, the activity of the Ba/Al_2O_3 catalyst was unaffected by added CO_2 and, moreover, always exceeded that of pure Al_2O_3 (Fig. 7). Consistent with this behavior, the C 1s region in the XPS spectrum of this catalyst showed no evidence for a carbonate species, indicating that a $BaCO_3$ phase was not formed, possibly due to the high surface area (Table 1) and acidic nature of the γ-Al_2O_3 support. Alternatively, the pretreatment of Ba/Al_2O_3 at 800°C may generate a $BaAl_2O_4$ spinel phase or some other non-basic Ba-containing mixed oxide that does not adsorb CO_2.

The C_2 product selectivities over these catalysts were relatively insensitive to total

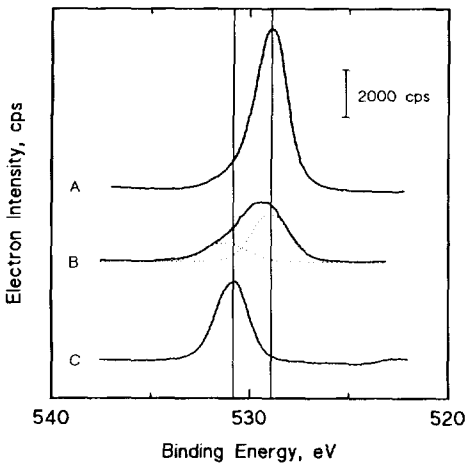

FIG. 9. XPS spectra in the O 1*s* region after treatment in oxygen at 800°C for 10 h: (A) MgO, (B) 4 mol% Ba/MgO, and (C) $BaCO_3$.

CO_2 partial pressure (Fig. 8). Carbon dioxide may affect the catalysts in two ways. First, it can convert the active Ba species (probably a BaO_2 phase, as suggested by the XPS results discussed below) into inactive $BaCO_3$, causing a decrease in both the activity and the C_2 selectivity. Second, CO_2 can poison the non-selective surface sites which are responsible for converting $CH_3\cdot$ radicals into CO_x. The combined result of these two effects may be seen in Figs. 5 and 8. For more highly basic catalysts (e.g., higher Ba loadings) the first effect dominates, and a net decrease in the C_2 selectivity with increasing CO_2 pressure is observed (Fig. 5). When the catalyst is less basic (0.5, 1 and 2 mol% Ba loadings), the second effect dominates at low CO_2 partial pressures, resulting in slight increases in the C_2 selectivity. However, with further increases in CO_2 pressures, BaO_2 is increasingly converted into $BaCO_3$, causing decreases in both activity and C_2 selectivity.

XPS and ISS Characterization of Ba/MgO Catalysts

Additional insight into the nature and distribution of surface species on the Ba/MgO catalysts was provided by XPS and ISS characterizations. Figures 9 and 10 contain typical XPS spectra in the O 1*s* and C 1*s* regions for pure MgO and $BaCO_3$, as well as for a representative Ba/MgO catalyst (4 mol% Ba), following initial pretreatment in O_2 at 800°C. Corresponding spectra for the same catalysts after exposure to a $CH_4 : O_2 : He = 5 : 1 : 6$ reaction mixture for 1 h at 800°C are shown in Figs. 11 and 12. Prior to spectral analysis, the used samples were cooled to ambient temperature in an $O_2 : He = 1 : 6$ mixture to remove reaction-generated surface hydroxyl species. As detailed previously, the presence of such hydroxyls prevents accurate determination of surface peroxides (O_2^{2-}), since the two species have very similar O 1s binding energies (*20*). It is apparent from Fig. 9 that although MgO and $BaCO_3$, as expected, each contain only a single type of oxygen species, the initial treatment in O_2 at 800°C results in the formation of more than one type of near-surface oxygen species on the Ba/MgO catalyst. The peak at ~529 eV in spectrum A and in the deconvoluted spectrum B is due to the O^{2-} species in MgO (and BaO, if present), while that at ~531 eV (in the absence of surface hydroxyls) may contain contributions from oxygen in both $BaCO_3$ and BaO_2 (peroxide). Although the latter two oxygen

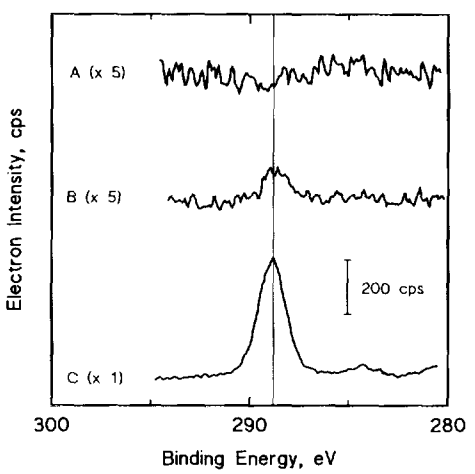

FIG. 10. XPS spectra in the C 1*s* region after treatment in oxygen at 800°C for 10 h: (A) MgO, (B) 4 mol% Ba/MgO, and (C) $BaCO_3$.

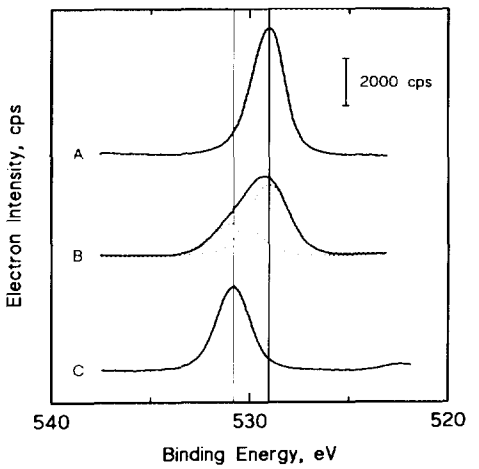

FIG. 11. XPS spectra in the O 1*s* region after exposure to a $CH_4:O_2:He = 5:1:6$ reaction mixture at 800°C for 1 h and subsequent cooling in O_2: He to 25°C: (A) MgO, (B) 4 mol% Ba/MgO, and (C) $BaCO_3$.

species were not resolvable in the O 1s region for any of the Ba/MgO compositions studied, their surface concentrations could nevertheless be individually obtained by measuring the area of the C 1*s* peak at ~289 eV (Fig. 10) to separately determine the amount of carbonate. Using the C : O = 1 : 3 stoichiometry of the carbonate species, the contribution due to CO_3^{2-} was then subtracted from the total area of the O 1*s* peak at ~531 eV to obtain the separate contribution due to O_2^{2-}. Table 3 summarizes the near-surface composition, determined using the above technique, of each Ba/MgO catalyst, both before and after exposure to the $CH_4:O_2:He$ reaction mixture.

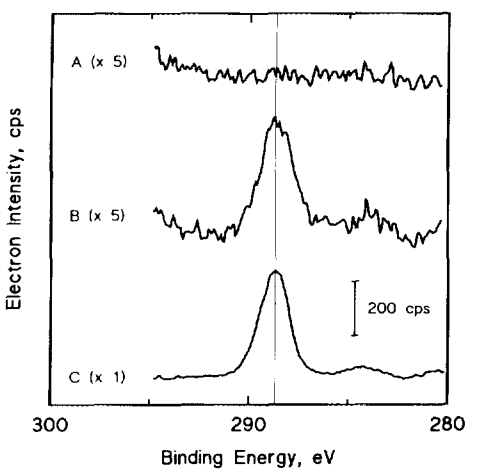

FIG. 12. XPS spectra in the C 1*s* region after exposure to a $CH_4:O_2:He = 5:1:6$ reaction mixture at 800°C for 1 h and subsequent cooling in O_2: He to 25°C: (A) MgO, (B) 4 mol% Ba/MgO, and (C) $BaCO_3$.

Following initial pretreatment in O_2 at 800°C, the near-surface barium in samples containing low Ba loadings (up to 4 mol%) existed primarily in the form of the peroxide. At higher loadings, however, an increasing fraction of the barium occurred as the carbonate, resulting from exposure of the synthesized catalysts to atmospheric carbon dioxide during handling, although a substantial amount of surface peroxide remained, even on the sample containing 25 mol% Ba. Exposure to the $CH_4:O_2:He$ reaction mixture at 800°C generated increased amounts of $BaCO_3$ for all Ba/MgO compositions, but the effect was most pronounced for those catalysts containing high Ba loadings (> 4 mol%). In agreement with the XPS results in Table 3, ion scattering spectra obtained for the 2 mol% Ba/MgO catalyst (Fig. 13) revealed that both the freshly pretreated sample and the one used for the $CH_4:O_2$ reaction contained only trace amounts of surface carbon. However, after being exposed to a reaction mixture in which CO_2 was added to the feed stream, the ISS spectrum of the sample contained a large scattering peak due to surface carbon, and the corresponding XPS spectrum (not shown) exhibited substantial increases in the intensities of the O 1*s* and C 1*s* peaks due to $BaCO_3$. This behavior is consistent with the results of the CO_2 poisoning experiments shown in Fig. 4, which indicate that the methane oxidation activities of Ba/MgO compositions having Ba contents exceeding ca. 1 mol% are very susceptible to poisoning by even small amounts of CO_2 in the reactant stream. The XPS and ISS results confirm that this poisoning is due to the formation of surface carbonate species, and that the poisoning effect is approximately proportional to the Ba loading of the cata-

TABLE 3

Surface Compositions of Ba/MgO Catalysts (mol%)

Catalyst (mol% Ba)	Oxygen			Carbon		Magnesium Mg^{2+}	Barium Ba^{2+}
	O_2^{2-}	CO_3^{2-}	O^{2-}	CO_3^{2-}	C		
Following initial treatment in O_2 at 800°C for 10 h							
0.0	0.0	0.0	57.8	0.0	0.0	42.2	0.0
0.2	10.1	0.0	49.2	0.0	0.0	38.6	2.1
0.5	11.5	0.5	46.1	0.2	0.0	37.8	3.9
1.0	13.4	0.5	44.5	0.2	0.0	38.4	3.0
2.0	16.9	0.6	43.0	0.2	0.0	35.1	4.2
4.0	18.4	1.1	40.1	0.4	0.0	34.8	5.2
8.0	13.9	7.4	38.6	2.5	0.0	31.8	5.8
15.0	19.1	26.2	15.5	8.7	0.0	10.8	19.7
25.0	15.2	44.1	1.9	14.7	0.0	0.0	24.1
Following exposure to $CH_4:O_2:He = 5:1:6$ reaction mixture at 800°C for 1 h							
0.2	8.0	0.5	52.6	0.2	0.0	36.6	2.1
0.5	10.4	2.3	47.2	0.8	0.0	36.3	3.0
1.0	10.9	2.5	46.6	0.8	0.0	35.8	3.4
2.0	16.9	3.4	38.9	1.1	0.0	34.7	5.0
4.0	17.0	3.3	41.0	1.1	0.0	33.5	4.1
8.0	13.0	14.8	30.7	4.9	0.0	27.7	8.9
15.0	5.3	52.2	0.0	17.4	0.0	0.0	25.1
25.0	5.1	53.1	0.0	17.7	0.0	0.0	24.1

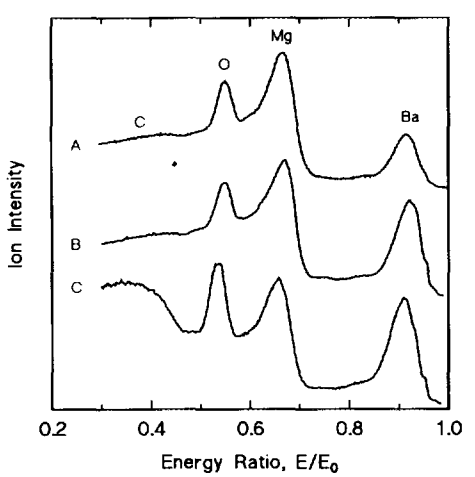

FIG. 13. ISS spectra of 2 mol% Ba/MgO: (A) after treatment in O_2 at 800°C 10 h, (B) after exposure to a $CH_4:O_2:He = 5:1:6$ reaction mixture at 800°C for 1 h and subsequent cooling in $O_2:He$ to 25°C, and (C) after exposure to $CH_4:O_2:He:CO_2 = 5:1:6:1$ reaction mixture at 800°C for 1 h and subsequent cooling in $O_2:He$ to 25°C.

lyst. Carbonate formation is not limited to the near-surface region of these materials, since XRD analysis of the 4 mol% Ba/MgO composition after exposure to the $CH_4:O_2$ reaction mixture at 800°C indicated the presence of only $BaCO_3$ and MgO, as well as a small amount of BaO_2 in the bulk of this used catalyst.

Further evidence supporting the above conclusion is provided by the CO_2 poisoning behaviors of the CaO-, ZnO-, and Al_2O_3-supported barium catalysts. XPS analysis revealed that, unlike the case for 2 mol% Ba/MgO (Table 3), most of the barium on the 2 mol% Ba/CaO catalyst remained in the form of $BaCO_3$ after exposure to the $CH_4:O_2:He$ reaction mixture. Correspondingly, the activity of this catalyst for methane oxidation was relatively unaffected by addition of CO_2 to the reactant mixture (Fig. 7), since most of the barium was already in the form of $BaCO_3$. By contrast, addition of carbon dioxide to the reactant stream

over the 2 mol% Ba/ZnO catalyst caused extensive loss of oxidation activity (Fig. 7), in agreement with XPS spectra for this material, which indicated the presence of relatively little $BaCO_3$ on the used sample. All surface carbonate formation detected by XPS on both of these catalysts must be due to $BaCO_3$ since, as shown in Fig. 1, $CaCO_3$ is not stable under these conditions, and the thermal stability of $ZnCO_3$, although not shown in Fig. 1, resembles that of $MgCO_3$. In the case of the 4 mol% Ba/Al_2O_3 catalyst, both XPS and TPD analyses indicated no formation of a carbonate species, even when carbon dioxide was present in the gas phase, and consequently the oxidation activity of this material was unaffected by the addition of CO_2 to the reactant mixture (Fig. 7). The possible presence of surface peroxide species on this catalyst could not be unambiguously determined, since, unlike the case for the other oxide supports studied, the O 1s binding energy of O^{2-} in Al_2O_3 (531.6 eV) is very similar to that of O_2^{2-} in BaO_2 (~531 eV).

Nature of the Active Sites

Previous studies by several investigators have been directed toward identification of the surface sites that are responsible for oxidative coupling of methane over various oxide-based catalysts (*13, 14, 21, 22, 24, 27*). Most of the catalysts that exhibit both high activity and high C_{2+} selectivity for this reaction may be classified as solid bases, e.g., pure and promoted alkaline earth oxides, lanthanide oxides, etc. However, as shown in previous studies (*22, 27*) and by the present investigation, correlations between activity/selectivity and inherent catalyst basicity, as measured by strength of CO_2 adsorption, for example, are not well defined. Based on our XPS determinations of the Ba/MgO surface compositions, it is likely that the sites on which selective activation of methane occurs involve a surface oxygen species. Figure 14 depicts graphically the effect of Ba loading on surface compositions of the used Ba/MgO catalysts, as summarized in Table 3. After exposure to the $CH_4 : O_2 :$ He reaction mixture at 800°C, the concentration of $BaCO_3$ in the near-surface region remains very low at Ba loadings ≤4 mol%, but increases significantly at higher Ba loadings, while the amount of exposed MgO decreases correspondingly. By contrast, the capability of the used catalysts to form a surface peroxide species (when cooled in O_2) increases up to a Ba loading level of 2 to 4 mol%, but then decreases at higher Ba loadings. This maximum in O_2^{2-} concentration agrees well with the corresponding maxima in oxidation activity observed for the 4 mol% Ba/MgO catalyst (Fig. 2), suggesting that a surface peroxide phase is involved in methane activation. We have previously reported evidence for the involvement of surface O_2^{2-} species in selectively activating methane over $BaPbO_3$ and $BaBiO_3$ catalysts (*20*). Yamashita *et al.* have also observed a similar maximum in methane oxidation activity for Ba/La_2O_3 catalysts at a Ba loading of 15 mol% (*24*). They suggested that breakage of the O–O bond in the surface peroxide is facilitated by high dispersion (i.e., low loading) of Ba on the La_2O_3 support. Hence, we postulate that, at sufficiently low Ba loadings, for which the

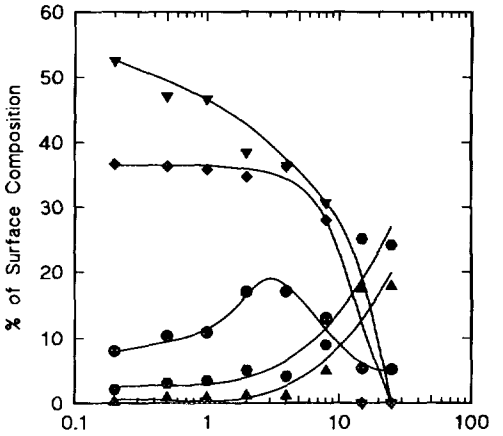

FIG. 14. Surface compositions of Ba/MgO catalysts after exposure to a $CH_4 : O_2 :$ He reaction mixture for 1 h at 800°C and subsequent cooling in $O_2 :$ He to 25°C. ▼, O^{2-}; ●, O_2^{2-}; ▲, CO_3^{2-}; ◆, Mg^{2+}; and , Ba^{2+}.

BaO_x remains uniformly distributed and well dispersed and $BaCO_3$ is more easily decomposed, oxidation activity initially increases with increasing Ba content. At higher Ba loadings, however, oxidation activity begins to decline with increasing Ba content, because of both decreased dispersion of the BaO_2 phase and increased thermal stability of the surface $BaCO_3$, as shown in Table 3 for the fresh catalysts.

Thus, for these oxide-based catalysts, the most significant correlation of methane oxidation activity/selectivity may be with their ability to form a reactive surface peroxide species, whose existence is sustained under reaction conditions only by the presence of molecular O_2 in the reactant stream. Although this tendency increases approximately with increasing catalyst basicity, the latter does not necessarily correlate with selective oxidation behavior. Over the range of Ba loadings from 0.2 to 4.0 mol%, for example, the concentration of surface carbonate, which may be taken as a measure of catalyst basicity, increases very little (Table 3); whereas, the catalytic activity increases markedly (Fig. 2). Pure $BaCO_3$ has virtually no intrinsic activity for methane coupling (Fig. 4) and acquires its apparent activity only after partial thermal decomposition into an active BaO_x phase. Finally, it should be noted that, although the correlation of methane oxidation activity with a surface peroxide species is clear, it is possible that the true active sites for methane activation may be O^- centers, which are generated by decomposition of O_2^{2-} entities. This conclusion is consistent with the postulate of Yamashita *et al.* (*24*) that oxidation activity is related to the ease of O–O bond breaking on the catalyst surface.

ACKNOWLEDGMENT

The authors gratefully acknowledge financial support of this research by the National Science Foundation under Grant CHE-9005808.

REFERENCES

1. Amenomiya, Y., Briss, V. I., Goledzinowski, M., Galuszka, J., and Sanger, A. R., *Catal. Rev.-Sci. Eng.* **32,** 163 (1990); Mackie, J. C., *Catal. Rev.-Sci. Eng.* **33,** 169 (1991).
2. Driscoll, D. J., Martir, W., Wang, J. X., and Lunsford, J. H., *J. Am. Chem. Soc.* **107,** 58 (1985).
3. Wang, J.-X., and Lunsford, J. H., *J. Phys. Chem.* **90,** 5883 (1986).
4. Zhang, H-S., Wang, J-X, Driscoll, D. J., and Lunsford, H. J., *J. Catal.* **112,** 366 (1988).
5. Campbell, K. D., Zhang, H., and Lunsford, J. H., *J. Phys. Chem.* **92,** 750 (1988).
6. Otsuka, K., and Jinno, K., *Inorg. Chim. Acta.* **121,** 237 (1986).
7. Otsuka, K., Murakami, Y., Wada, Y., Said, A. A., and Morikawa, A., *J. Catal.* **121,** 122 (1990).
8. Peng, X. D., Richards, D. A., and Stair, P. C., *J. Catal.* **121,** 99 (1990).
9. Peng, X. D., and Stair, P. C., *J. Catal.* **128,** 264 (1991).
10. Zhang, Z-L., Au, C. T., and Tsai, K. R., *Appl. Catal.* **62,** L29 (1990).
11. Badyal, J. P. S., Zhang, X., and Lambert, R. M., *Surf. Sci. Lett.* **225,** L15 (1990).
12. Otsuka, K., Jinno, K., and Morikawa, A., *Chem. Lett.*, 499 (1985).
13. Dubois, J-L., and Cameron, C. J., *Appl. Catal.* **67,** 49 (1990).
14. Maitra, A. M., Campbell, I., and Tyler, R. J., *Appl. Catal. A:General* **85,** 27 (1992).
15. Bytyn, W., and Baerns, M., *Appl. Catal.* **28,** 199 (1986).
16. Carreiro, J. A. S. P., and Baerns, M., *J. Catal.* **117,** 258 (1989).
17. Sokolovskii, V. D., Aliev, S. M., Buyevskaya, O. V., and Davydov, A. A., *Catal. Today* **4,** 293 (1989).
18. Tong, Y., Rosynek, M. P., and Lunsford, J. H., *J. Catal.* **126,** 291 (1990).
19. Kharas, K. C. C., and Lunsford, J. H., *J. Am. Chem. Soc.* **111,** 2336 (1989).
20. Dissanayake, D., Kharas, K. C. C., Lunsford, J. H., and Rosynek, M. P., *J. Catal.* **139,** 652 (1993).
21. Otsuka, K., Said, A. A., Jinno, K., and Komatsu, T., *Chem. Lett.*, 77 (1987).
22. Moneuse, C., Cassir, M., Piolet, C., and Devynck, J., *Appl. Catal.* **63,** 67 (1990).
23. Aika, K., Moriyama, T., Takasaki, N., and Iwamatsu, E., *J. Chem. Soc. Chem. Commun.*, 1210 (1986).
24. Yamashita, H., Machida, Y., and Tomita, A., *Appl. Catal. A:General* **79,** 203 (1991).
25. Dubois, J-L., Bisiaux, M., Mimoun, H., and Cameron, C. J., *Chem. Lett.* **6,** 967 (1990).
26. Remy, H. (Ed.), "Treatise on Inorganic Chemistry," Vol. 1. Elsevier, Amsterdam, 1956.
27. Sinev, M. Yu., Filkova, D. G., Bychkov, V. Yu, Ukharskii, A. A., and Krylov, O. V., *Kinet. Catal.* **32,** 137 (1991).